# Heat transfer analysis of Casson fluid

By:

**Irfan Ullah**
**Reg. No # 274-FBAS/MSMA/F15**

**Department of Mathematics & Statistics**
**Faculty of Basic & Applied Sciences**
**International Islamic University, Islamabad**
**Pakistan**
**2018**

1- Heat transfer Analysis

2- Elementary Heat transfer Analysis

# Heat transfer analysis of Casson fluid

By:

**Irfan Ullah**
**Reg. No # 274-FBAS/MSMA/F15**

Supervised By:

**Dr. Tariq Javed**

**Department of Mathematics & Statistics**
**Faculty of Basic & Applied Sciences**
**International Islamic University, Islamabad**
**Pakistan**

**2018**

# Heat transfer analysis of Casson fluid

By:

**Irfan Ullah**
**Reg. No # 274-FBAS/MSMA/F15**

**A DISSERTATION IN THE PARTIAL FULFILLMENT OF THE REQUIREMENTS FOR THE DEGREE OF THE MASTER OF SCIENCE IN MATHEMATICS**

Supervised By:

**Dr. Tariq Javed**

**Department of Mathematics & Statistics**
**Faculty of Basic & Applied Sciences**
**International Islamic University, Islamabad**
**Pakistan**
**2018**

# Certificate

# Heat transfer analysis of Casson Fluid

By

## Irfan Ullah

A DISSERTATION SUBMITTED IN THE PARTIAL FULFILLMENT OF THE REQUIREMENTS FOR THE DEGREE OF THE MASTER OF SCIENCE IN MATHEMATICS

**We accept this dissertation as conforming to the required standard.**

1. ______________________
***Prof. Dr. Masood Khan***
External Examiner

2. ______________________
**Dr. Nasir Ali**
Internal Examiner

3. ______________________
***Dr.Tariq Javed***
Supervisor

4. ______________________
**Prof. Dr. Muhammad Sajid, T.I**
Chairperson

**Department of Mathematics & Statistics**
**Faculty of Basic and Applied Sciences**
**International Islamic University, Islamabad**
**Pakistan**
**2018**

DEDICATED TO

MY FAMILY

# Declaration

I hereby declare that this thesis, neither as a whole nor as a part thereof, has been copied out from any source. It is further declared that I have prepared this thesis entirely on the basis of my personal efforts made under the sincere guidance of my supervisor. No portion of the work, presented in thesis, has been submitted in the support of any application for any degree or qualification of this or any other institute of learning.

Signature: __________
**Irfan Ullah**
**Reg. No# # 274-FBAS/MSMA/F15**
Department of Maths and Stats
Faculty of Basic and Applied Sciences
International Islamic University, Islamabad,
Pakistan.

# Acknowledgement

To begin with the name of Almighty **ALLAH,** the creator of the universe, who bestowed his blessing on me to complete this dissertation. I offer my humblest, sincerest and million Darood to the **Holy Prophet Hazrat MUHAMMAD (s.a.w)** who exhorts his followers to seek for knowledge from cradle to grave.

I wish to acknowledge the Tulane, kind help, valuable instructions, intellectual suggestions and beneficial remarks of my sincere and kind-hearted supervisor **Dr. Tariq Javed,** without his generous encouragement and patient guidance, it would have been difficult for me to complete the assigned task.

I owe my deep gratitude and heartfelt thanks to my mother who supported me throughout my career and guided me at every step in my life. I always feel in debated to my sisters and wife for their special and profound prayers for my brilliant success. I thankful to my father and brothers **Faheemullah, Sehadullah and Faizanullauh** who patiently and smilingly provided me with all sort of facilities and kept on praying for me.

My acknowledgement will remain incomplete if I do not mention the companionship of my all friends especially **Dr. Abuzar, Dr. Irfan, Muhammad Arshad Siddiqui, Ziafat Mehmood, Bilal Ahmed, Abdul Haleem** and my beloved friends **Muhammad Shoaib, Muhammad Arif and Imtiaz Ali Shah** and my entire colleague for their help in my course and research work.

Last not least I am thankful to my sincere and honorable friend **Dr. Rahmat Ullah** for his unbeatable help and guidance to achieve my highest education

**Irfan Ullah**

# Preface

In the study of fluid mechanics, equations describing the boundary layer fluid flows along with the solution of such governing equation with the help of some suitable transformation are of great importance [1]. This is all due the boundary layer theory and application in fluid dynamics that various useful mathematical differential equations have been derived in due to study different. Since many fluids of industrial importance are of non-Newtonian type, therefore in this connection such fluids are highly degraded over Newtonian fluids. Generally, it is observed that in need life and industrial fluid application can be recognized by their usage in petroleum drilling, polymer engineering, certain separation processes manufacturing of foods and paper and some other industrial processes [2]. Therefore, such investigation of fluid flows cannot be neglected while dealing with the fluids in the fluid of fluid dynamics.

The term non-Newtonian fluid corresponds to various nonlinear relations among stress and strain therefore it is impossible express all the properties of various non-Newtonian fluids through single governing equation. Therefore, different models are there for non-Newtonian fluid [3]. One of such non-Newtonian fluids is Casson fluid. This fluid behave as elastic solid and Casson fluid corresponds to a yield shear stress in governing equation.

Crane [4] is known to be first to study time independent 2D flow of a non-Newtonian fluid caused by a stretching sheet that moves in its own plane having linearly variable velocity. The idea of Crane [4] was extended by many researchers to study various aspects of fluid and heat flow in a fluid of infinite extent surrounding a stretching sheet [5-16].

Some fluids like oil, water and ethylene glycol mixtures etc. do not transfer heat efficiently because of having low thermal conductivity. The thermal conductivity these fluids may be enhanced through suspension of normalized particle materials. Main characteristic feature of the nanofluid is thermal conducting enhancement [17].

Chapter 1 consists some basic definition and prerequisites [5] for the convenience and better understanding of the reader. Chapter 2 is a review of study presented by Raj Nandkeolyar [18]. This chapter explains the investigation of heat and mass transfer through nanofluid over a stretching sheet with homogeneous-heterogeneous reactions. Numerical solution of this problem is obtained using BVP4C. Chapter 3 is a review of investigation presented by Bhattacharyya [19] to analysis heat flow through Casson fluid close to stagnation point over a stretching sheet. Numerical solution for this investigation are obtained using shooting method.

# Contents

# Chapter 1

## 1.1 Fluids

A substance which occupied no fixed shape and deforms easily due to external pressure is known as fluid.

## 1.2 Flow

A phenomenon showing the continuous deformation when subject to the applied forces is said to be flow.

## 1.3 Properties of fluid

### 1.3.1 Density

Amount of mass in a unit volume is termed as density. The mathematical form of density $\rho$ at a point is

$$\rho = \lim_{v \to 0} \left(\frac{m}{v}\right) \tag{1.1}$$

### 1.3.2 Pressure

The normal force $F$ acting on surface $S$ per unit area is termed as pressure. Mathematically, the pressure $p$ is defined as

$$p = \lim_{S \to 0} \left(\frac{F}{S}\right). \tag{1.2}$$

### 1.3.3 Viscosity

The frictional force between any two adjacent layers of a fluid which opposes the motion of one layer over other is known as viscosity of that fluid.

Mathematically, viscosity $\mu$ is defined as

$$\mu = \frac{\mathcal{T}_{yx}}{du/dy}. \quad (1.3)$$

### 1.3.4 Kinematic viscosity

Ratio of viscosity to the density is termed as Kinematic. Mathematically,

$$\nu = \frac{\mu}{\rho}. \quad (1.4)$$

## 1.4 Types of Fluid

The fluids are of generally two types which are explained as follows:

### 1.4.1 Ideal fluid

A fluid with no viscosity or negligible viscosity ($\mu = 0$) is said to be on ideal fluid.

### 1.4.2 Real fluid

A fluid whose viscosity is not equal to zero ($\mu \neq 0$) is known as real fluid. It is also called viscous fluid and denoted by $\mu$. Real fluid has two major branches.

(1) Newtonian fluid
(2) Non-Newtonian fluid

### 1.4.3 Newtonian fluid

If stress is linearly proportional to strain then such fluid is known as Newtonian fluid, e.g. water, oil and alcohol etc. Mathematically, this relationship is written as

$$\mathcal{T}_{yx} \propto \frac{du}{dy}$$

$$\mathcal{T}_{yx} = \mu \frac{du}{dy}. \quad (1.5)$$

where $\mu$ is constant of proportionality.

### 1.4.4 Non-Newtonian fluid

If stress is not linearly proportional to strain then such fluid is known as Newtonian fluid, e.g. shampoo, paint and blood etc. The mathematical expression of non-Newtonian fluid is

$$\mathcal{T}_{yx} = \eta\left(\frac{du}{dy}\right)^{n}, \; (n \neq 1) \tag{1.6}$$

## 1.5 Types of flow

The nature of fluid flow can be categorized in following types.

### 1.5.1 Compressible flow

If the density of flowing fluid changes with the position then such a fluid flow is said to be compressible flow. Flow of gases is the most common example of compressible flow.

### 1.5.2 Incompressible flow

If the density of the fluid remain constant throughout the motion then such a fluid flow is termed as incompressible flow. The example of incompressible flow is the flow of liquids.

### 1.5.3 Steady flow

If the properties of the fluid in the domain are not changing with respect to time, then such fluid flow is said to exhibit steady flow. Mathematically, it can be represented as

$$\frac{\partial q}{\partial t} = 0. \tag{1.7}$$

where $q$ represents any property of the fluid.

### 1.5.4 Unsteady flow

If flow properties time dependent then such flow is said to be unsteady flow. Mathematically, it can be written as

$$\frac{\partial q}{\partial t} \neq 0. \tag{1.8}$$

### 1.5.5 Laminar flow

The flow of a fluid in which layers of fluid slide smoothly past each other or remains parallel to each other is called laminar flow or stream line flow. The pattern of laminar flow is shown in the figure below.

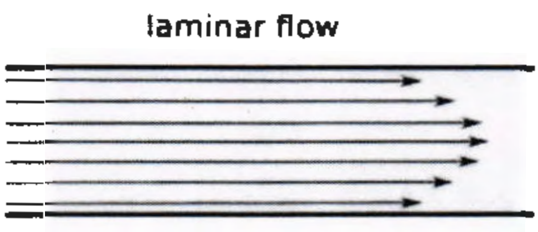


### 1.5.6 Turbulent flow

The flow of a fluid in which there is great disorder and the layer's of fluid does not slide smoothly past each other is called turbulent flow. The pattern of turbulent flow is shown in the figure below.

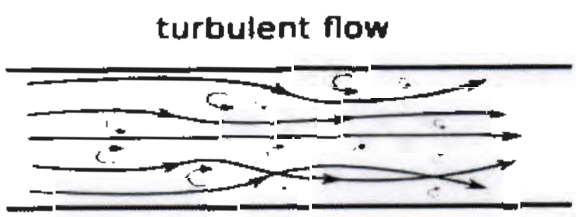


## 1.6 Temperature

Measure of the average heat in a substance is known as temperature.

## 1.7 Heat

Heat is a form of energy which flows either between a system and its surrounding or within a system by virtue of a temperature difference.

## 1.8 Modes of Heat transfer

The heat transfer from one place to another through following modes:

### 1.8.1 Conduction

The process by which heat energy is transferred from particle to another particle by collision is called conduction. The mode of heat transfer usually occurs in solids.

### 1.8.2 Convection

The process in which heat is transferred from one place to another due to transfer of molecules the substance is called convection. This phenomenon appears in liquid and gasses.

### 1.8.3 Radiation

The process in which heat is transferred from one place to another without any material medium is known as radiation. Visible light is the example of radiation.

## 1.9 Continuity equation

Law of conservation of mass may be represented through continuity equation given as follows

$$\frac{\partial \rho}{\partial t} + \nabla.(\rho V) = 0. \tag{1.9}$$

Following form of above equation is obtained by considering flow incompressible i.e. density do not depend upon time or space or is assumed constant

$$\nabla.V = 0. \tag{1.10}$$

Above equation may be represented as follows in cylindrical coordinate system

$$\frac{\partial u}{\partial z}+\frac{1}{r}\frac{\partial (vr)}{\partial r}+\frac{1}{r}\frac{\partial w}{\partial \phi}=0, \tag{1.11}$$

where $u$, $v$ and $w$ corresponds to the components of velocity along x y and z directions.

## 1.10 Energy equation

Heat transfer in fluids may be studied through energy equation which is modeled with help of first law of thermodynamics. Following form of energy equation is obtained in rectangular coordinate system

$$u\frac{\partial T}{\partial x}+v\,\frac{\partial T}{\partial y}+w\,\frac{\partial T}{\partial z}=\left(\frac{k}{pc_p}\right)\left[\frac{\partial^2 T}{\partial x^2}+\frac{\partial^2 T}{\partial y^2}+\frac{\partial^2 T}{\partial z^2}\right]+\left(\frac{\mu}{pc_p}\right)\varphi, \tag{1.12}$$

here, we may define dissipation function as follows in 3D case

$$\varphi=2\left[\left(\frac{\partial u}{\partial x}\right)^2+\left(\frac{\partial v}{\partial y}\right)^2+\left(\frac{\partial w}{\partial z}\right)^2\right]+\left[\frac{\partial u}{\partial y}+\frac{\partial v}{\partial x}\right]^2+\left[\frac{\partial w}{\partial y}+\frac{\partial v}{\partial z}\right]^2+\left[\frac{\partial u}{\partial z}+\frac{\partial w}{\partial x}\right]^2 \tag{1.13}$$

Above equation may take following form in cylindrical coordinate system

$$u\frac{\partial T}{\partial z}+v\,\frac{\partial T}{\partial r}+\frac{w}{r}\frac{\partial T}{\partial \varphi}=\left(\frac{k}{pc_p}\right)\left[\frac{\partial^2 T}{\partial z^2}+\frac{1}{r}\frac{\partial}{\partial r}\left(r\frac{\partial T}{\partial r}\right)+\frac{1}{r^2}\frac{\partial^2 T}{\partial \varphi^2}\right]+\left(\frac{\mu}{pc_p}\right)\varphi, \tag{1.14}$$

here the cylindrical form of dissipation function may be expressed as follows

$$\varphi=2\left[\left(\frac{\partial u}{\partial z}\right)^2+\left(\frac{\partial v}{\partial r}\right)^2+\left(\frac{1}{r}\frac{\partial w}{\partial \varphi}+\frac{v}{r}\right)^2\right]+\left[\frac{1}{r}\frac{\partial u}{\partial \varphi}+\frac{\partial w}{\partial z}\right]^2+\left[\frac{\partial v}{\partial z}+\frac{\partial u}{\partial r}\right]^2+ \left[\frac{1}{r}\frac{\partial v}{\partial \varphi}+\frac{\partial w}{\partial r}-\frac{w}{r}\right]^2. \tag{1.15}$$

## 1.11 The momentum equation

The momentum equation of motion is given by

$$\rho \frac{\partial \boldsymbol{T}}{\partial t} = div\boldsymbol{T} + \rho \boldsymbol{b}, \tag{1.16}$$

***T*** and ***b*** being stress tensor and body force respectively. Further stress tensor ***T*** is given as

$$\mathrm{T}=\begin{bmatrix} \mathcal{J}_{xx} & \mathcal{J}_{xy} & \mathcal{J}_{xz} \\ \mathcal{J}_{yx} & \mathcal{J}_{yy} & \mathcal{J}_{yz} \\ \mathcal{J}_{zx} & \mathcal{J}_{zy} & \mathcal{J}_{zz} \end{bmatrix}, \tag{1.17}$$

where $\mathcal{J}_{xx}$, $\mathcal{J}_{yy}$ and $\mathcal{J}_{zz}$ represents normal stresses and $\mathcal{J}_{xy}$, $\mathcal{J}_{xz}$, $\mathcal{J}_{zy}$ are called shear stress.

## 1.12 Runge-Kutta method of order 4.

Suppose second order IVP is given by

$$\frac{d^2y}{dx^2} = f\left(x, y, \frac{dy}{dx}\right), \qquad [\,a\,,b\,] \tag{1.18}$$

subject to the initial conditions are

$$y(a) = \alpha, \qquad \frac{dy}{dx}(a) = \beta. \tag{1.19}$$

To solve the above equation, we have need to change the 2nd order IVP into the system of two 1st order IVP. For this, we introduce z as follows

$$\left.\begin{aligned} \frac{dy}{dx} &= z = g(x, y, z) \\ \frac{dz}{dx} &= f(x, y, z) \end{aligned}\right\}. \tag{1.20}$$

Now equation (1.19) become

$$y(a) = \alpha, \qquad z(a) = \beta. \tag{1.21}$$

Solution of equation (1.20) with initial conditions Eq. (1.21) can be calculated absolutely through formula [16]

$$y_{n+1} = y_n + \frac{1}{6}(q_1 + 2q_2 + 2q_3 + q_4), \tag{1.22}$$

$$z_{n+1} = z_n + \frac{1}{6}(p_1 + 2p_2 + 2p_3 + p_4), \tag{1.23}$$

where

$$\left.\begin{aligned} q_1 &= hg(x_n, y_n, z_n), \\ p_1 &= hf(x_n, y_n, z_n), \\ q_2 &= hg\left(x_n + \frac{h}{2}, y_n + \frac{q_1}{2}, z_n + \frac{p_1}{2}\right), \\ p_2 &= hf\left(x_n + \frac{h}{2}, y_n + \frac{q_1}{2}, z_n + \frac{p_1}{2}\right), \\ q_3 &= hg\left(x_n + \frac{h}{2}, y_n + \frac{q_2}{2}, z_n + \frac{p_2}{2}\right), \\ p_3 &= hf\left(x_n + \frac{h}{2}, y_n + \frac{q_2}{2}, z_n + \frac{p_2}{2}\right), \\ q_4 &= hg(x_n + h, y_n + q_3, z_n + p_3), \\ p_4 &= hf(x_n + h, y_n + q_3, z_n + p_3). \end{aligned}\right\} \tag{1.24}$$

$n$ and $h$ are number of steps and size of steps respectively defined as $t = \frac{b-a}{n}$.

## 1.13 Shooting method

Consider the two-point BVP as follows,

$$y'' = f(x, y, y'), \qquad [a, b] \tag{1.25}$$

Subject to boundary conditions

$$\begin{aligned} y(a) &= \alpha \\ y(b) &= \beta. \end{aligned} \tag{1.26}$$

This method involves replacing of BVP into system of first order initial value problem. In this method, we solve the IVP,

$$y'' = f(x, y, y'), \tag{1.27}$$

with initial condition

$$y(a) = a, \qquad y'(a) = s^{(i)}. \tag{1.28}$$

Where $s^{(i)}$ is some approximation of the initial slope. Using any of the methods for solving the above IVP, the approximation $y^{(1)}(b)$ to the solution $y(b)$ is determined. This value is either smaller or larger than the required solution $y(b) = \beta$. Let us denote,

$$g(s^{(0)}) = y^{(1)}(b) - y(b) = y^{(1)}(b) - \beta. \qquad (1.29)$$

Where $s^{(0)}$ is the first approximation of $s^{(i)}$. If $g(s^{(0)}) = 0$, then the condition at $x = b$ is satisfied. If this condition is not satisfied, then we repeat the above procedure using $y'(x) = s^{(1)}$ to find another estimate $y^{(2)}(b)$ for $y(b)$. The process is usually repeated until the computed value at $x = b$ agree with the boundary condition $y(b) = \beta$. Depending on the choice of $y'(b)$, the computed solution may over shoot or under shoot the required solution.

The shooting method may be described as a procedure which defines a functional relationship $g(s^{(i)}) = 0$, between $y(b)$ and the slope $y'(b)$. The problem is then to find the root of this equation, i.e. $g(s^{(i)}) = 0$. The secant method can be used for the value of $s^{(i)}$,

$$s^{(n+1)} = s^{(n)} - \left[\frac{s^{(n)} - s^{(n-1)}}{g(s^{(n)}) - g(s^{(n-1)})}\right]\left(g(s^{(n)}) - b\right) \qquad n = 1,2,3, \ldots \qquad (1.30)$$

If the differential equation is linear, then shooting method becomes very simple. It can be shown that the functional relationship $g(s^{(i)}) = 0$ between $y'(b)$ and $y(b)$ is also linear.

# Chapter 2

# Heat and Mass transfer analysis in nanofluid flow over a stretching sheet with homogeneous-heterogeneous reactions

Present chapter is related to study the effects of homogeneous-heterogeneous reactions on the heat transfer through nanofluid with internal heat generation source done by Raj Nandkeolayar *et al* [18]. The flow under consideration is also under the effect of externally applied magnetic field. Raj Nandkeolayar *et al* [18] are the responsible for presenting this intuitive idea by considering the copper and gold particle and ended up with obtaining an exact solution in the form of hypergeometric functions. Moreover, a numerical solution has also been sought, by using BVP4c, in order to make an in-depth look into the considered problem.

## 2.1 Mathematical Modeling

Let us assume the two-dimension, incompressible steady flow of nanofluid with viscous fluid as a base fluid over a stretching sheet with heat generation. The fluid is assumed as electrically conducting. Consider the sheet is placed in the *xz*-plane and *y* is perpendicular to the plane. Two forces with same magnitude but opposite in direction are exerted along the sheet to keep the wall stretched and origin location is fixed. The fluid flow is passed through a uniform strong the magnetic field and it is assumed that the induced magnetic field is very small and hence ignorable in comparison of applied magnetic field [7]. The fluid has a water based nanofluid that includes copper or gold, chemically denoted as (Cu) and (Au) respectively. Nanoparticles and the base fluid exhibit thermal equilibrium state and no slip is present between them. We considered that a homogeneous and heterogeneous reactions model occurs as investigated in [6] is given respectively by

$$A + 2B \rightarrow 3B, \qquad rate = k_c a b^2 \tag{2.1}$$

and

$$A \rightarrow B, \qquad rate = k_s a. \tag{2.2}$$

Here $a$ and $b$ being concentration of the chemical species $A$ and $B$, $k_c$ and $k_s$ are constants. Equations of governing flow problem are as follow:

$$\frac{\partial u}{\partial x}+\frac{\partial v}{\partial y}=0\,, \tag{2.3}$$

$$u\frac{\partial u}{\partial x}+v\frac{\partial u}{\partial y}=\frac{\mu_{nf}}{\rho_{nf}}\frac{\partial^2 u}{\partial y^2}-\frac{\sigma\beta_0^2}{\rho_{nf}}u\,, \tag{2.4}$$

$$u\frac{\partial T}{\partial x}+v\frac{\partial T}{\partial y}=\alpha_{nf}\frac{\partial^2 T}{\partial y^2}+\frac{Q_0}{(\rho c_p)_{nf}}(T-T_\infty)\,, \tag{2.5}$$

$$u\frac{\partial a}{\partial x}+v\frac{\partial a}{\partial y}=D_A\frac{\partial^2 a}{\partial y^2}-k_c a b^2\,, \tag{2.6}$$

$$u\frac{\partial b}{\partial x}+v\frac{\partial b}{\partial y}=D_B\frac{\partial^2 b}{\partial y^2}+k_c a b^2\,, \tag{2.7}$$

with boundary conditions

$$\left.\begin{array}{c} u=u_w=cx, \quad v=0, \quad T=T_W=T_\infty+C\left(\frac{x}{l}\right)^2 \\ D_A\frac{\partial a}{\partial y}=k_s a, \quad D_B\frac{\partial b}{\partial y}=-k_s a \quad at \quad y=0 \\ u\to 0, \quad T=T_\infty, \quad a\to a_0, \quad b\to 0 \quad as \quad y\to\infty \end{array}\right\}. \tag{2.8}$$

The nanofluid dynamics viscosity given by Brinkman [14] is

$$\mu_{nf}=\frac{\mu_f}{(1-\phi)^{2.5}}\,, \tag{2.9}$$

where $\phi$ being solid volume fraction. The effective density of nanofluid is defined as

$$\rho_{nf}=(1-\phi)\rho_f+\phi\rho_s\,, \tag{2.10}$$

and thermal diffusivity is

$$\alpha_{nf}=\frac{k_{nf}}{(\rho c_p)_{nf}}\,, \tag{2.11}$$

where $k_{nf}$ being thermal conductivity and $(\rho c_p)_{nf}$ being heat capacitances and define as

$$\frac{k_{nf}}{k_f}=\frac{k_s+2k_f-2\phi(k_f-k_s)}{k_s+2k_f+2\phi(k_f-k_s)}\,, \tag{2.12}$$

$$\left(\rho c_p\right)_{nf} = (1-\phi)(\rho c_p)_f + \phi(\rho c_p)_s\,, \tag{2.13}$$

Here the index corresponds to thermal characteristics of $nf$= nanofluid, $f$ = base fluid and $s$ = nanosolid particles. Eq. (2.3) is automatically satisfied by nominating a stream function $\Psi(x,y)$ which satisfies the usual velocity stream function relation.

where $\Psi = (c\nu_f)^{\frac{1}{2}} x f(\eta)$, $f(\eta)$ is nondimensional stream function and $\eta = (\frac{c}{\nu_f})^{\frac{1}{2}} y$. The velocity components can be define as

$$u = cxf'(\eta) \qquad \text{and} \qquad v = -(c\nu_f)^{\frac{1}{2}} f(\eta) \tag{2.14}$$

nanofluid's temperature is given by

$$T = T_\infty + (T_w - T_\infty)\theta(\eta)\,. \tag{2.15}$$

Chemical species $A$ and $B$ have the concentration which is mathematically given by

$$a = a_o g(\eta) \qquad \text{and} \qquad b = a_o h(\eta) \tag{2.16}$$

where $a_o$ is a constant, $\theta(\eta)$ is the nondimensional temperature, and $g(\eta)$ & $h(\eta)$ are nondimensional concentrations. From equations (2.9)-(2.16), equations (2.4)-(2.8) in nondimensional form simplify to the two-point BVPs as follows

$$f''' + \phi_1\left(ff'' - \frac{M}{\phi_2}f' - f'^2\right) = 0, \tag{2.17}$$

$$\theta'' + Pr\frac{k_f}{k_{nf}}\phi_3\left(f\theta' - 2f'\theta + \frac{\beta}{\phi_3}\theta\right) = 0, \tag{2.18}$$

$$\frac{1}{Sc}g'' + fg' - kgh^2 = 0, \tag{2.19}$$

$$\frac{\delta}{Sc}h'' + fh' + kgh^2 = 0, \tag{2.20}$$

with BCs

$$\left.\begin{array}{l} f(0)=0, \quad f'(0)=1, \quad f'(\eta)\to 0 \quad as\ \eta\to\infty \\ \theta(0)=1, \quad \theta(\eta)\to 0 \quad as \quad \eta\to\infty \\ g'(0)=k_s g(0), \quad g(\eta)\to 1 \quad as\ \eta\to\infty \\ \delta h'(0)=-k_s g(0), \quad h(\eta)\to 0 \quad as\ \eta\to\infty \end{array}\right\} . \tag{2.21}$$

where

$$\phi_1=(1-\phi)^{2.5}\left\{(1-\phi)+\phi\left(\frac{\rho_s}{\rho_f}\right)\right\} \tag{2.22}$$

$$\phi_2=\left\{(1-\phi)+\phi\left(\frac{\rho_s}{\rho_f}\right)\right\} \tag{2.23}$$

$$\phi_3=\left\{(1-\phi)+\frac{(\rho c)_s}{(\rho c_p)_f}\phi\right\} \tag{2.24}$$

The nondimensional constants in equations, (2.17)-(2.21) are $M$, $Pr$, $\delta$, $\beta$, $Sc$, $k$ and $Ks$ represent magnetic parameter, Prandtl number, ratio of diffusion coefficients, heat generation, Schmidt number, strength of the homogeneous reaction and strength of the heterogeneous reaction respectively. These are defines as

$$\begin{array}{llll} M=\frac{\sigma B_0{}^2}{\rho_f c}, & \beta=\frac{Q_0}{c(\rho c_p)_f}, & Pr=\frac{(\rho\upsilon c_p)_f}{k_f}, & Sc=\frac{\upsilon_f}{D_{\bar{A}}}, \\ \delta=\frac{D_{\bar{B}}}{D_{\bar{A}}}, & k=\frac{k_c a_0{}^2}{c}, & K_s=\frac{k_s}{D_{\bar{A}}}\sqrt{\frac{\upsilon_f}{c}} . & \end{array} \tag{2.25}$$

Here $\bar{A}$ and $\bar{B}$ are of equivalent size which implies that $D_{\bar{A}}$ and $D_{\bar{B}}$ are also equal, i.e., $\delta=1$ [6]. This supposition yield following equation,

$$g(\eta)+h(\eta)=1 . \tag{2.26}$$

Eq. (2.19) and Eq. (2.20) under this supposition reduce to

$$\frac{1}{Sc}g''+fg'-kg(1-g)^2=0, \tag{2.27}$$

with following BCs

$$g'(0)=K_s g(0), \quad g(\eta)\to 1 \quad as \quad \eta\to\infty. \tag{2.28}$$

## 2.2.1 Solution of momentum equation

The energy and species equation are decoupled by momentum boundary layer equation. On integrating equation (2.17) in terms of $\eta$ over the interval $[0,\ \eta]$ with the boundary condition (2.21) will give the following exact solution

$$\mathrm{f}(\eta) = \frac{1-e^{-s\eta}}{s} \ . \tag{2.29}$$

where $s$ being parameter related with nanoparticle volume fraction, fluid density, nanoparticle density and magnetic field parameter. This will satisfy the Eq. given by

$$s = \sqrt{\phi_1 + (1-\phi)^{2.5}M}. \tag{2.30}$$

It should be highlighted that for $\phi$ to be zero, Eq. (2.30) reduce to $s = \sqrt{1+M}$, which are presented by [4].

## 2.2.2 Solution of heat exchange equation

We define the following variable,

$$\xi = -\frac{Pr}{s^2} e^{-s\eta}. \tag{2.31}$$

Eq. (2.18) and thermal BCs (2.21) will become

$$\xi g_{\xi\xi} + [1 - \lambda_1(Pr^* + \xi)]g_\xi + \frac{1}{\xi} Pr^* \lambda\beta_g = 0, \tag{2.32}$$

$$g(-Pr^*) = 1, \qquad g(0) \rightarrow 0, \tag{2.33}$$

where $Pr^* = \frac{Pr}{s^2}$ being modified Prandtl number. Result obtained from Eq. (2.32) in the form of hypergeometric functions which is given below,

$$g(\xi) = C_0 \xi^\alpha F[\alpha, 1+n, \lambda_1 \xi], \tag{2.34}$$

where

$$F[m,n,z] = \sum_{r=0}^{\infty} \frac{m(m+1)......(m+r-1)z}{n(n+r)......(n+r-1)r!}$$

Upon using the boundary condition (2.33) and expressing result in terms of independent variable, we have

$$g(\eta) = \frac{e^{-s\eta\alpha}F[\alpha,\ 1+n,\ -\lambda_2 e^{-s\eta}]}{F[\alpha,\ 1+n,\ -\lambda_2]}. \tag{2.35}$$

Rate of surface heat exchange is obtained in the form of

$$g'(0) = \frac{\left(\frac{\alpha}{1+n}\right)F[\alpha+1,\ 2+n,\ -\lambda_2]-s\alpha F[\alpha,\ 1+n,-\lambda_2]}{F[\alpha,\ 1+n,\ -\lambda_2]}, \tag{2.36}$$

where

$$\alpha = \frac{m+n}{2}, \qquad \lambda = \frac{k_f}{k_{nf}}, \qquad \lambda_1 = \lambda\phi_2, \qquad \lambda_2 = \lambda_1 Pr *.$$

### 2.2.3 Skin friction coefficient

The quantity which is physically quite appealing is $C_f$, that gives the surface drag. The shearing stress $\tau_w$ is defined as

$$\tau_w = -\mu_{nf}\left[\frac{\partial u}{\partial y}\right]_{y=0} = -\frac{1}{(1-\phi)^{2.5}}\rho_f\sqrt{\upsilon_f C^3}xf'''(0) \tag{2.37}$$

where $\mu_{nf}$ being viscosity coefficient. The skin friction coefficient is given by

$$C_f = \frac{2\tau_w}{\rho_f {u_w}^2}, \tag{2.38}$$

Upon using Eq. (2.37) in equation (2.38), we get

$$C_f(1-\phi)^{2.5}\sqrt{Re_x} = -2f''(0), \tag{2.39}$$

where $Re_x$ is said to be local Reynolds number and is defined by $Re_x = xu_w/\upsilon_f$.

### 2.2.4 Coefficient of heat transfer

The rate of heat exchange at the wall can be defined as

$$q_w = -k_{nf}\left[\frac{\partial T}{\partial y}\right]_{y=0} = -k_{nf}C\left(\frac{x}{l}\right)^2\sqrt{\frac{c}{\upsilon_f}}\theta'(0). \tag{2.40}$$

The Nusselt number is defined as

$$Nu_x = \frac{xq_w}{k_f(T_w - T_\infty)} \tag{2.41}$$

and using equation (2.40) in equation (2.41), the dimensional rate of heat exchange at wall is obtained as

$$\frac{Nu_x}{\sqrt{Re_x}}\left(\frac{k_f}{k_{nf}}\right) = -\theta'(0)\,. \tag{2.42}$$

## 2.7 Graphical results

### 2.7.1 Tables

**Table 2.1:** Thermo physical characteristics of water and nano-particles.

| | $\rho(kg/m^3)$ | $C_p(j/kgK)$ | $k\ (W/mK)$ |
|---|---|---|---|
| Pure water | 997.1 | 4179 | 0.613 |
| Copper water(Cu) | 8933 | 385 | 401 |
| Gold (Au) | 19282 | 129 | 310 |

**Table 2.2:** A comparison of exiting $-f''(0)$ due to Cu-water nano-fluid against various values of $M$ and $\phi$ when $\Pr = 6.2$ with that of Hamad [5] and Kameswaran *et al.* [16]

| M | $\phi$ | Hamad[5] | Kameswaran *et al.* [16] | Our results |
|---|---|---|---|---|
| 0 | 0.05 | 1.10892 | 1.108919904 | 1.1089199038 |
| | 0.1 | 1.17475 | 1.174746021 | 1.1747460214 |
| | 0.15 | 1.20886 | 1.208862320 | 1.2088623198 |
| | 0.2 | 1.21804 | 1.218043809 | 1.2180438095 |
| 0.5 | 0.05 | 1.29210 | 1.292101949 | 1.2921019495 |
| | 0.1 | 1.32825 | 1.328248829 | 1.3282488285 |
| | 0.15 | 1.33955 | 1.339553714 | 1.3395537136 |
| | 0.2 | 1.33036 | 1.330356126 | 1.3303561264 |
| 1 | 0.05 | 1.45236 | 1.452360679 | 1.4523606792 |
| | 0.1 | 1.46576 | 1.465763175 | 1.4657631753 |
| | 0.15 | 1.45858 | 1.458581570 | 1.4585815696 |
| | 0.2 | 1.43390 | 1.433898227 | 1.4338982265 |
| 2 | 0.05 | 1.72887 | 1.728872387 | 1.7288723875 |
| | 0.1 | 1.70789 | 1.707892022 | 1.7078920216 |
| | 0.15 | 1.67140 | 1.671398302 | 1.6713983015 |
| | 0.2 | 1.62126 | 1.621264175 | 1.6212641754 |

**Table 2.3:** A comparison of calculated local Nusselt number $-\theta'(0)$ due to Cu-water nano-fluid for different values of Pr with that of Grubka and Bobba [15] and Kameswaran [16]

| Result | $Pr = 0.72$ | $Pr = 1.0$ | $Pr = 3.0$ | $Pr = 10$ | $P_r = 100$ |
|---|---|---|---|---|---|
| Grubka & Bobba [15] | 1.0885 | 1.3333 | 2.5097 | 4.7969 | 15.7120 |
| Kameswaran *et al.* [16] | 1.08852 | 1.33333 | 2.50973 | 4.79687 | 15.71163 |
| Our results | 1.088524 | 1.333333 | 2.509725 | 4.796873 | 15.711967 |

**Table 2.4:** Calculated numerical value of $-f''(0)$ and $-\theta'(0)$ for different values of magnetic parameter $M$, heat generation parameter $\beta$ and solid volume fraction $\phi$ when $k = K_s = 1$ and $Sc = 5$

| | | | Cu-water | | Au-water | |
|---|---|---|---|---|---|---|
| M | $\beta$ | $\phi$ | $-f''(0)$ | $-\theta'(0)$ | $-f''(0)$ | $-\theta'(0)$ |
| 1 | 0.1 | 0.1 | 1.46576318 | 3.10463489 | 1.71639926 | 2.98796095 |
| 2 | 0.1 | 0.1 | 1.70789202 | 3.03362162 | 1.92729341 | 2.92395300 |
| 3 | 0.1 | 0.1 | 1.91972098 | 2.96973231 | 2.11728443 | 2.86467942 |
| 2 | 0.15 | 0.1 | ----- | 2.98338556 | ----- | 2.86876051 |
| 2 | 0.2 | 0.1 | ----- | 2.93155781 | ----- | 2.81089758 |
| 2 | 0.1 | 0.0 | 1.73205081 | 3.60882094 | 1.73205081 | 3.60882094 |
| 2 | 0.1 | 0.1 | 1.70789202 | 3.03362162 | 1.92729341 | 2.92395300 |
| 2 | 0.1 | 0.2 | 1.62126418 | 2.58126309 | 1.95635457 | 2.39868695 |

### 2.7.2 Graphical representation

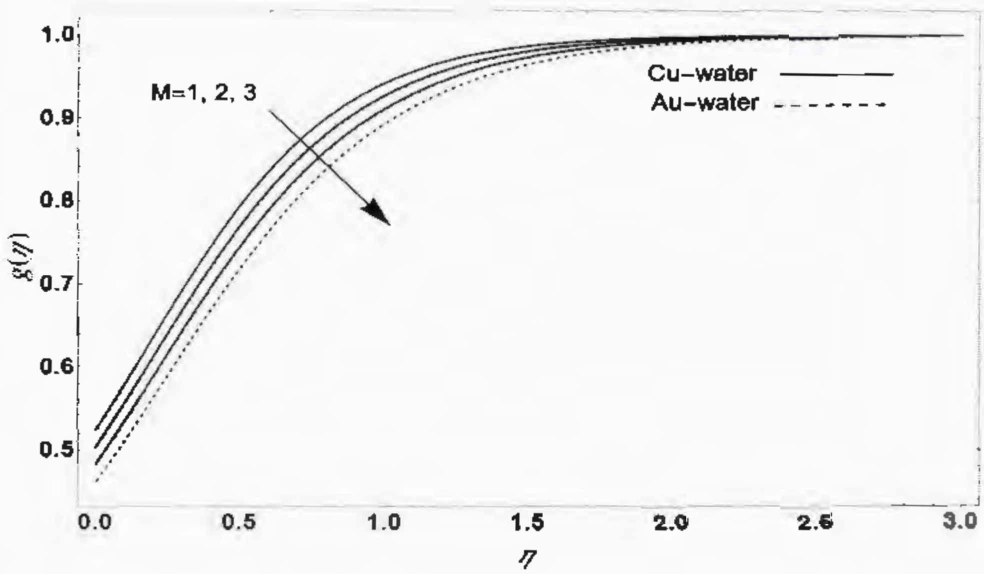


**Figure 2.1:** Graphical view of the effects due to $M$ on the species concentration given by $g(\eta)$ when $Sc = 5,\ k = 1,\ K_s = 1,\ \phi = 0.1$.

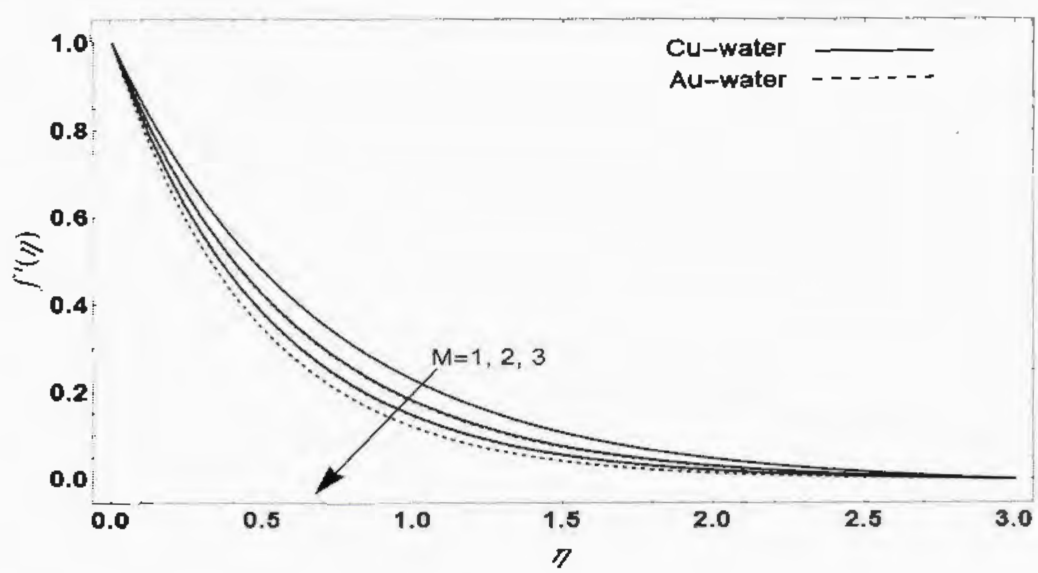


**Figure 2.2:** Graphical view of the effects due to $M$ on the nanofluid velocity given by $f'(\eta)$ when $\phi = 0.1$.

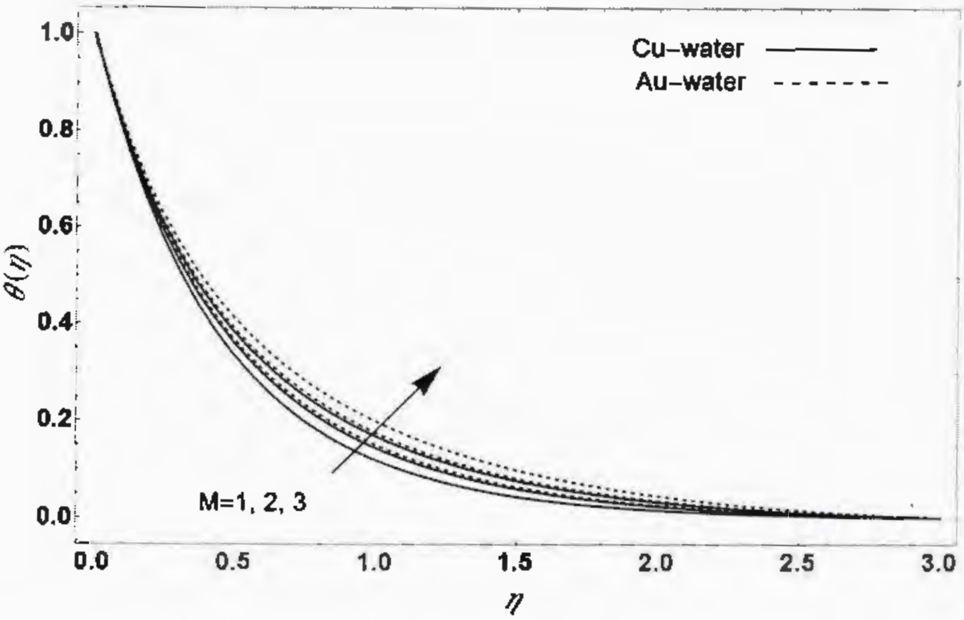


**Figure 2.3:** Graphical view of the effects due to $M$ on the temperature given by $\theta(\eta)$ when and $\beta = 0.1$.

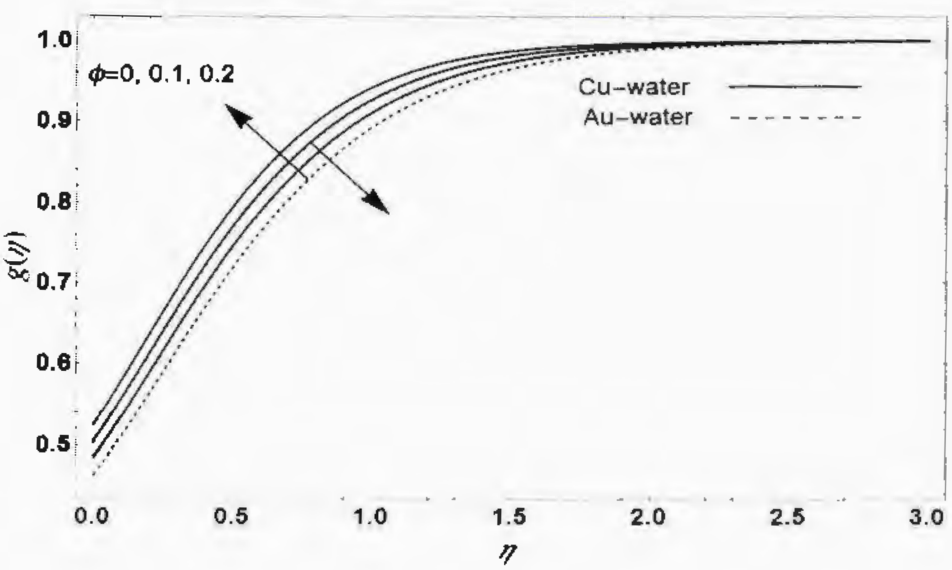


**Figure 2.4:** Graphical view of the effects due to $\phi = 0.1$ on the species concentration given by $g(\eta)$ when $Sc = 5,\ k = 1,\ Ks = 1,\ M = 2$.

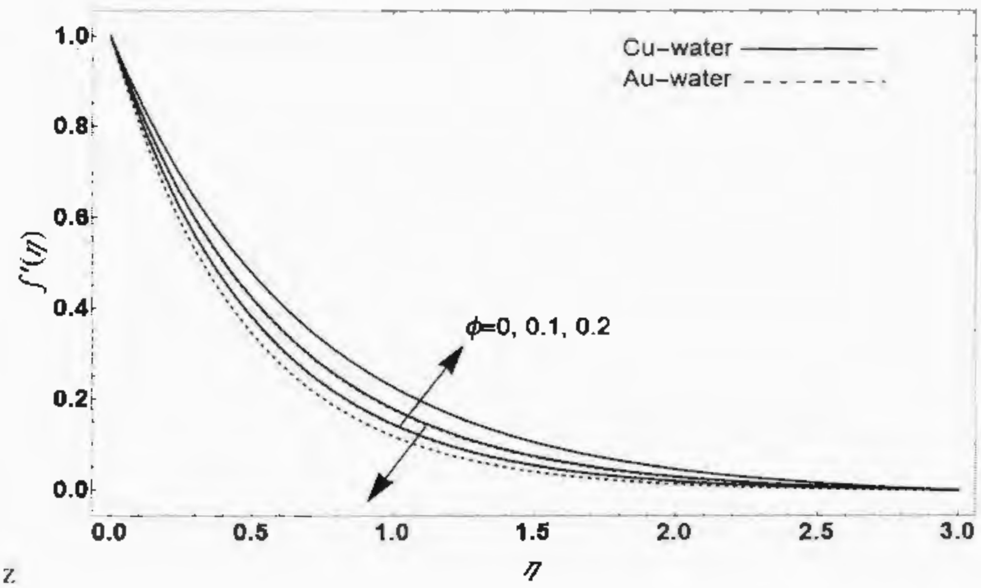


**Figure 2.5:** Graphical view of the effects due to $\phi$ on the nanofluid velocity given by $f'(\eta)$ when $M = 2$.

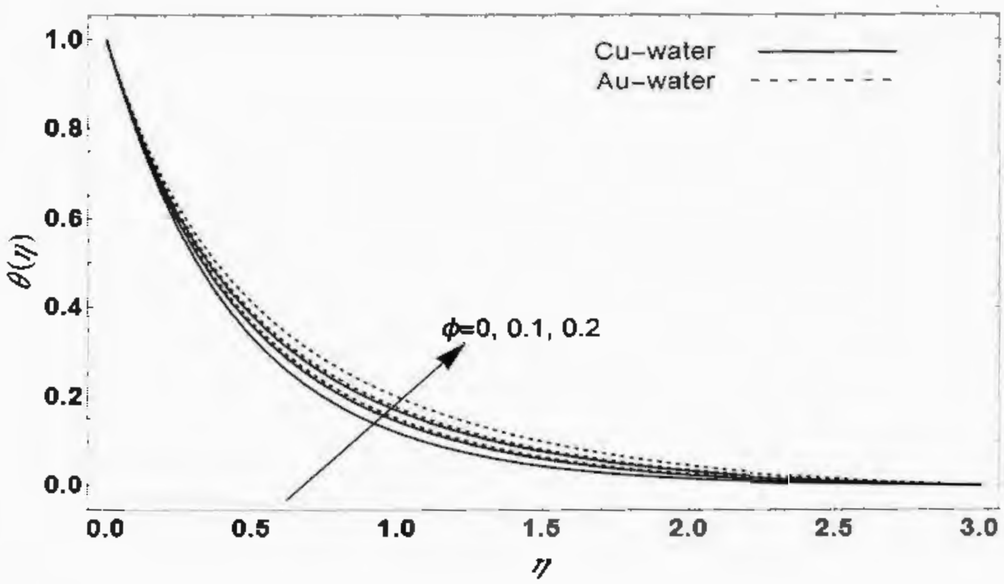


**Figure 2.6:** Graphical view of the effects due to $\phi$ on the nanofluid temperature given by $\theta(\eta)$ when $M = 2$ and $\beta = 0.1$.

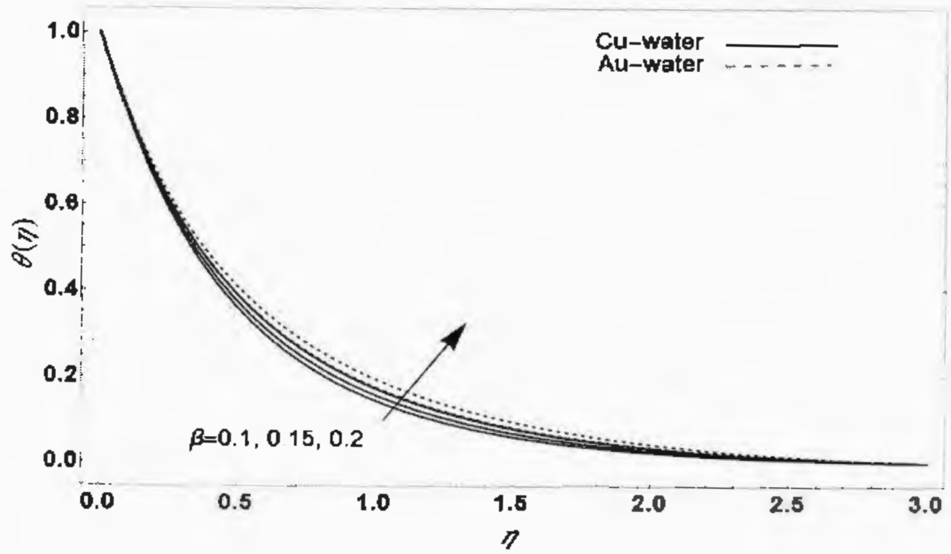


**Figure 2.7:** Graphical view of the effects due to $\beta$ on the nanofluid temperature given by $\theta(\eta)$ when $M = 2$ and $\phi = 0.1$.

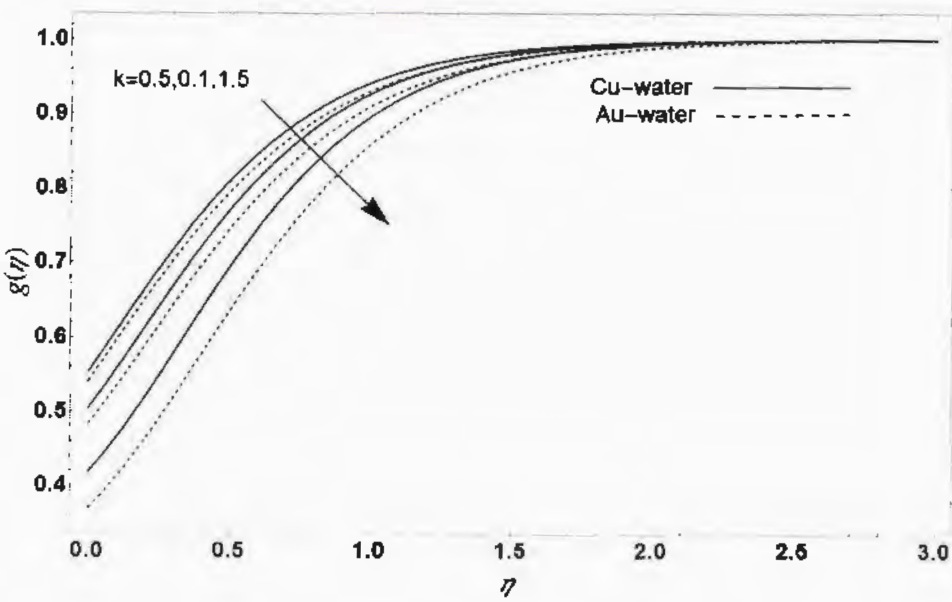


**Figure 2.8:** Graphical view of the effects shown by $k$ on the species concentration given by $g(\eta)$ when $Sc = 5,\ \phi = 0.1,\ Ks = 1,\ M = 2$.

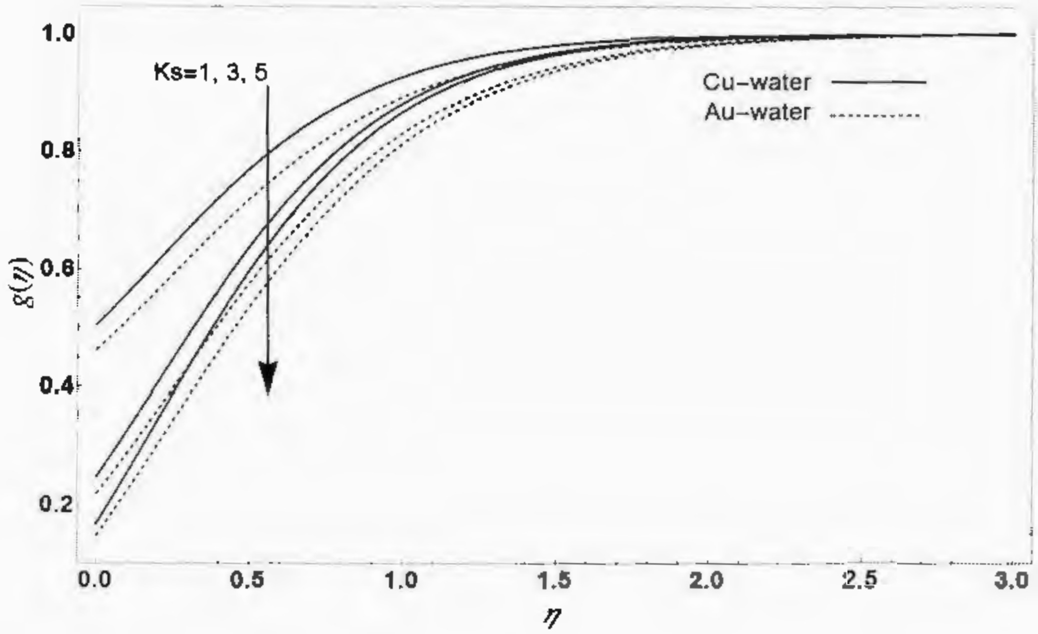


**Figure 2.9:** Graphical view of the effects shown by$Ks$ on the species concentration given by $g(\eta)$ when $Sc = 5,\ \phi = 0.1,\ k = 1,\ M = 2.$

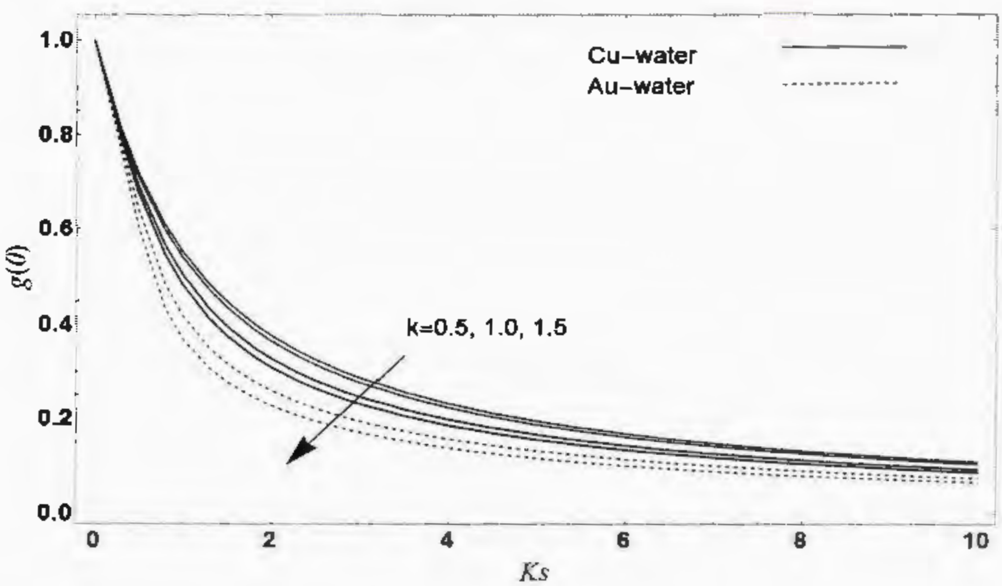


**Figure 2.10:** Graphical view of the effects due to $k$ and $Ks$ on the species concentration at surface given by $g(0)$ when $Sc = 5,\ \phi = 0.1,\ M = 2.$

## 2.8 Results and Discussion

The solution of the boundary value problem modeled in term of coupled non-linear ordinary differential equations (2.17) – (2.20) subject to BCs (2.21) is obtained by using shooting method for various values assigned to the magnetic parameters $M$, solid volume fraction parameter $\phi$, heat generation parameter $\beta$, strength of homogeneous and heterogeneous reactions are presented by $k$ and $Ks$ respectively. Table 2.2 gives the comparison of the values of computed skin friction coefficient $-f''(0)$ with the results presented is [5] and [16]. Table 2.3 is constructed to show the comparison of computed local nusselt number $-\theta'(0)$ with the results available in [15] and [16] for various values of $Pr$. Table 2.4 represents skin friction coefficient $-f''(0)$ and heat transfer rate $-\theta'(0)$ for various flow parameters $M, \beta$ and $\phi$. It is noted from the table 2.4 that due to increase in the value of $M$, the increase in $-f''(0)$ and decrease in $-\theta'(0)$ is noted for both Au-water and Cu-water nanofluids. Figures 2.1-2.10 depict the profile of fluid velocity $f'(\eta)$, fluid temperature $\theta(\eta)$, and species concentration $g(\eta)$ for different assigned values of the involved parameters. Figures 2.1-2.3 show the variation of species concentration $g(\eta)$, fluid temperature $\theta(\eta)$ and nanofluid velocity $f'(\eta)$ due to magnetic parameter $M$. It is observed from these figures that the magnetic parameter $M$ effect is inversely proportional to the species concentration $g(\eta)$ and fluid velocity $f'(\eta)$, where fluid temperature $\theta(\eta)$ is directly proportional to the effect of magnetic parameter $M$. It is because of the reason that the resistance force appear in the flow field due to presence of magnetic field. Figures 2.4- 2.6 show the variation of species concentration $g(\eta)$, fluid temperature $\theta(\eta)$ and fluid velocity $f'(\eta)$ for different values of solid volume fraction $\phi$. Increases in the value of solid volume fraction $\phi$ increases the fluid temperature $\theta(\eta)$ for both Cu-water and Au-water. It is noted that species concentration $g(\eta)$ and fluid velocity $f'(\eta)$ increases in Cu-water for increasing solid volume fraction $\phi$ while decreasing in Au-water for increasing solid volume fraction $\phi$. Moreover the concentration boundary layer thickness increases for Cu-water and decreases for Au-water with increasing nanoparticles. Figure 2.7 show the variation of fluid temperature $\theta(\eta)$ for various values of heat generation $\beta$. It is clearly observed that fluid temperature $\theta(\eta)$ rises with rise in the values of heat generation $\beta$. Figures 2.8 and 2.9 show the impacts of the intensity of the homogeneous reaction denoted by $k$ and heterogeneous reaction denoted by $K_s$ on the concentration of species $g(\eta)$. We observed that the increase in the value of $k$ and $K_s$ increases the species concentration $g(\eta)$ as can be seen in figure 2.10.

# Chapter 3

# Heat transfer analysis in Casson fluid near a stagnation point over a stretching/shrinking sheet

## 3.1 Introduction

In this chapter, we focus the investigation of boundary layer flow of heated Casson fluid towards the stagnation point over a shrinking/stretching sheet [19]. The governing partial differential equations are converted into set of ordinary differential equations with the help of similarity transformation. Then the transformed nonlinear boundary value problem in term of ordinary differential equations has been tackled by *"Shooting method"* in order to seek a reliable and approximate solution of the given problem. The effects of some important parameters and variables are displayed graphically and discussed in detail.

## 3.2 Mathematical construction of the problem

Consider steady of incompressible and two-dimensional flow of Casson fluid over a shrinking/stretching sheet near the point of stagnation represented by the region $0 \leq y < \infty$. The flow of such isotropic and incompressible type of fluids has exquisitely been described by the relation given by Nakamura [12] as follows

$$\tau_{ij} = \begin{cases} (\mu_\beta + \frac{p_y}{\sqrt{2\pi}})2e_{ij} & \pi > \pi_c \\ (\mu_\beta + \frac{p_y}{\sqrt{2\pi_c}})2e_{ij} & \pi < \pi_c \end{cases} \tag{3.1}$$

Where $\mu_B$ being plastic dynamic viscosity, $p_y$ is fluid stress, $\pi$ is the product of component of rate of deformation, namely $\pi = e_{ij}e_{ij}$, $e_{ij}$ being the (I, j)-th component of the rate of deformation and $\pi_c$ is critical value of $\pi$ based on non-Newtonian form.

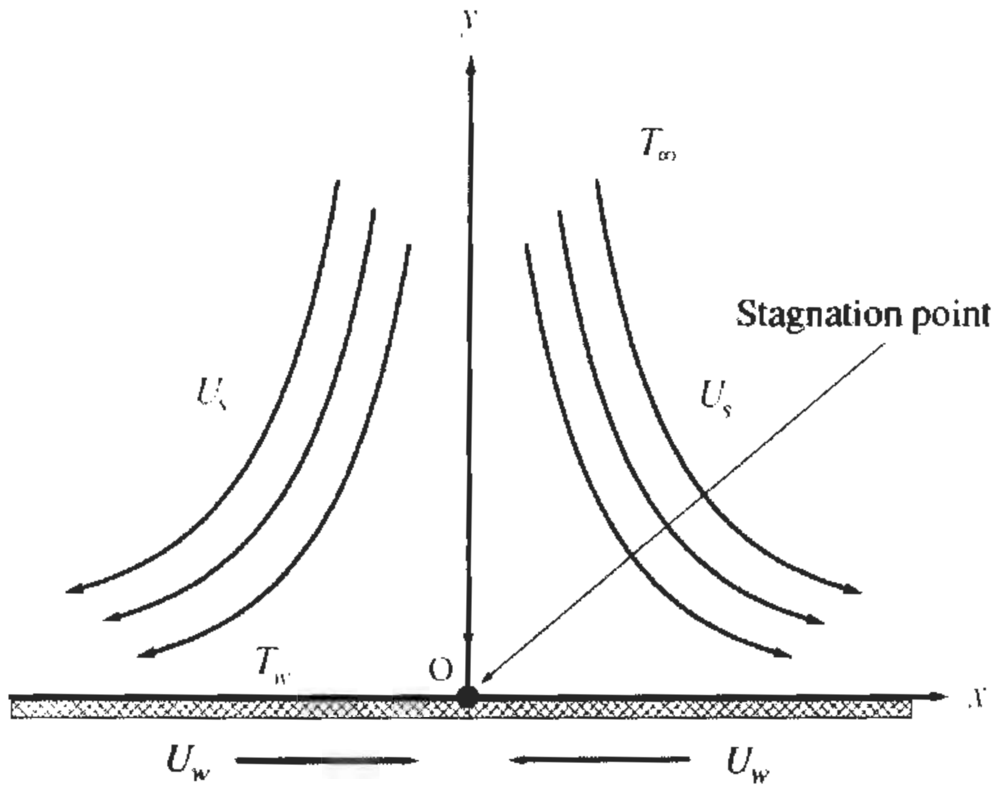


**Fig. 3.1:** Geometry of problem

The following governing equations describe the above flow model

$$\frac{\partial u}{\partial x}+\frac{\partial v}{\partial y}=0, \tag{3.2}$$

$$u\frac{\partial u}{\partial x}+v\frac{\partial v}{\partial y}=U_s\frac{dU_s}{dx}+\upsilon\,(1+1/\beta)\frac{\partial^2 u}{\partial y^2}, \tag{3.3}$$

where $u$ and $v$ being velocity components along the $x$-direction and $y$- direction, $U_s = ax$ being straining velocity, $\upsilon$ being kinematic fluid viscosity and $\beta = {}^{\mu_B\sqrt{2\pi_c}}/_{p_y}$ being non-Newtonian parameter. The BCs for the problem are given by

$$u = U_w,\quad v = 0,\ \text{ at } y = 0;\ u \to U_s \quad \text{ as } \ y \to \infty \tag{3.4}$$

where $U_w = cx$ is shrinking/stretching velocity of the sheet. The shrinking and stretching cases are studied through $c > 0$ and $c < 0$ respectively.

By using the velocity-stream function relationship

$$u = \frac{\partial \Psi}{\partial y}, \qquad v = -\frac{\partial \Psi}{\partial x} \tag{3.5}$$

$\Psi$ being the stream function, the Eq. (3.2), is automatically satisfied and Eq. (3.3) becomes

$$\frac{\partial \Psi}{\partial y}\frac{\partial^2 \Psi}{\partial x \partial y} - \frac{\partial \Psi}{\partial x}\frac{\partial^2 \Psi}{\partial y^2} = U_s \frac{dU_s}{dx} + v\left(1 + \frac{1}{\beta}\right)\frac{\partial^3 \Psi}{\partial y^3}, \tag{3.6}$$

The boundary conditions reduce to

$$\frac{\partial \Psi}{\partial y} = U_w, \qquad \frac{\partial \Psi}{\partial x} = 0 \text{ at } \quad y = 0; \quad \frac{\partial \Psi}{\partial y} \to U_S \quad \text{as} \quad y \to \infty \tag{3.7}$$

The introduced nondimensional variable for the stream function is

$$\Psi = \sqrt{av}xf(\eta) \tag{3.8}$$

where $\eta$ represents the similarity variable that can be written as $\eta = y\sqrt{a/v}$.

Upon using Eq. (3.8) and the similarity variable, the equation (3.6) is given by

$$\left(1 + \frac{1}{\beta}\right)f''' + ff'' - f'^2 + 1 = 0\,, \tag{3.9}$$

where prime sign denote derivative w. r. to $\eta$.The boundary condition now simplify

$$\begin{gathered} f(\eta) = 0, \quad f'(\eta) = c/a \qquad at \qquad \eta = 0, \\ f'(\eta) \to 1 \qquad as \quad \eta \to \infty\,. \end{gathered} \tag{3.10}$$

Now by considering the distribution of temperature in the flow field, the principle energy equation is given by

$$u\frac{\partial T}{\partial x} + v\frac{\partial T}{\partial y} = \frac{\kappa}{\rho c_p}\frac{\partial^2 T}{\partial y^2}\,, \tag{3.11}$$

where $T$, $\rho$, $\kappa$, and $c_p$ being temperature, fluid density, thermal conductivity and specific heat respectively. The boundary conditions for the problem are given by

$$T = T_w, \quad at \quad y = 0; \quad T \to T_\infty, \quad as \quad y \to \infty\,, \tag{3.12}$$

where $T_w$ is constant temperature and $T_\infty$ is constant free stream temperature.

The non-dimensional temperature $\theta$ is defined as

$$\theta(\eta) = \frac{T-T_\infty}{T_w-T_\infty}. \quad (3.13)$$

Using Eq. (3.8), Eq. (3.13) and the similarity variable $\eta$, the Eq. (3.11) finally takes the following form:

$$\theta'' + Prf\theta' = 0. \quad (3.14)$$

Here primes indicates derivative in term of $\eta$ and $Pr = c_p\mu/\kappa$ represents the Prandtl number. The boundary condition from Eq. (3.12) now become

$$\theta(\eta) = 0, \quad at \quad \eta = 0, \theta(\eta) \to 0, \quad as \quad \eta \to \infty \quad (3.15)$$

## 3.3 Numerical solution of the problem

Since the exact solution to non-linear, coupled differential given in Eqs. (3.9) and (3.14) hardly possible. Therefore, in order to obtain the solution of it, the numerical approach has been taken into account. In this confection, a well-known numerical method namely shooting method has been used to achieve an approximate solution to the above given non-linear boundary value problem by converting the boundary value problem to initial value problem. Thus the system of first order IVP is given as

$$\left.\begin{aligned} f &= y_1 \\ f' &= y_2 \\ f'' &= y_3 \\ y'_3 &= ((-y_1y_3 + (y_2)^2 - 1))/(1 + \tfrac{1}{\beta}) \\ \theta &= y_4 \\ \theta' &= y_5 \\ y'_5 &= -Pry_1y_5 \end{aligned}\right\}, \quad (3.16)$$

Subject to the following initial conditions

$$y_1(0) = 0,\ y_2(0) = c/a\ ,\ y_3(0) = s, \\ y_4(0) = 1,\ y_5(0) = t. \tag{3.17}$$

Where $s$ and $t$ are two unknown missing conditions. The missing conditions can be found in such a way that the solution satisfies the boundary conditions (3.10) and (3.15). We construct the solution of initial value problem represented by (3.16) with the help of Runge-kutta 4th order scheme. The missing constants $s$ & $t$ are iterated with the help of Newton- Rephson method and iterated up to the accuracy$10^{-5}$ . It is noted that the missing conditions and the value of infinity are highly dependenting on the physical parameters $\beta$, Pr and $^c/_a$.

## 3.4 Graphical results

### 3.4.1 Tables

**Table 3.1:** Comparison of Numerical values of $f''(0)$ obtained by the present scheme with that of Wang [10] and Ishak [11] for various values of *c/a* and for $\beta \to \infty$ for stretching sheet case



| c/a | Present study | Wang[10] | Ishak *et al.* [11] |
|---|---|---|---|
| 0 | 1.2325878 | 1.232588 | 1.232588 |
| 0.1 | 1.1465608 | 1.14656 | 1.146561 |
| 0.2 | 1.0511299 | 1.05113 | 1.051130 |
| 0.5 | 0.7132951 | 0.71330 | 0.713295 |
| 1 | 0 | 0 | 0 |

**Table 3.2:** Comparison of Numerical values of $f''(0)$ for first and second solution obtained by the present scheme with that of Wang [10] and Ishak [11] for various values of *c/a* and for $\beta \to \infty$ for stretching sheet case.

| *c/a* | Present study | | Wang[10] | | Ishak *et al.* [11] | |
|---|---|---|---|---|---|---|
| | 1st solution | 2nd solution | 1st solution | 2nd solution | 1st solution | 2nd solution |
| -0.25 | | | | | | |
| -0.5 | 1.4022405 | | 1.40224 | | 1.402241 | |
| -0.75 | 1.4956697 | | 1.49567 | | 1.495670 | |
| -1 | 1.4892981 | | 1.48930 | | 1.489298 | |
| -1.1 | 1.3288169 | 0 | 1.32882 | | 1.328817 | 0 |
| -1.15 | 1.1866806 | 0.0492286 | | | 1.186681 | 0.049229 |
| -1.2 | 1.0822316 | 0.1167023 | 1.08223 | 0.116702 | 1.082231 | 0.116702 |
| -1.24 | 0.9324728 | 0.2336491 | | | 0.932474 | 0.233650 |
| -1.2465 | 0.5842915 | 0.5542856 | 0.55430 | | 0.584295 | 0.554283 |
| -1.24657 | 0.5745268 | 0.5639987 | | | | |

### 3.4.2 Graphical Results

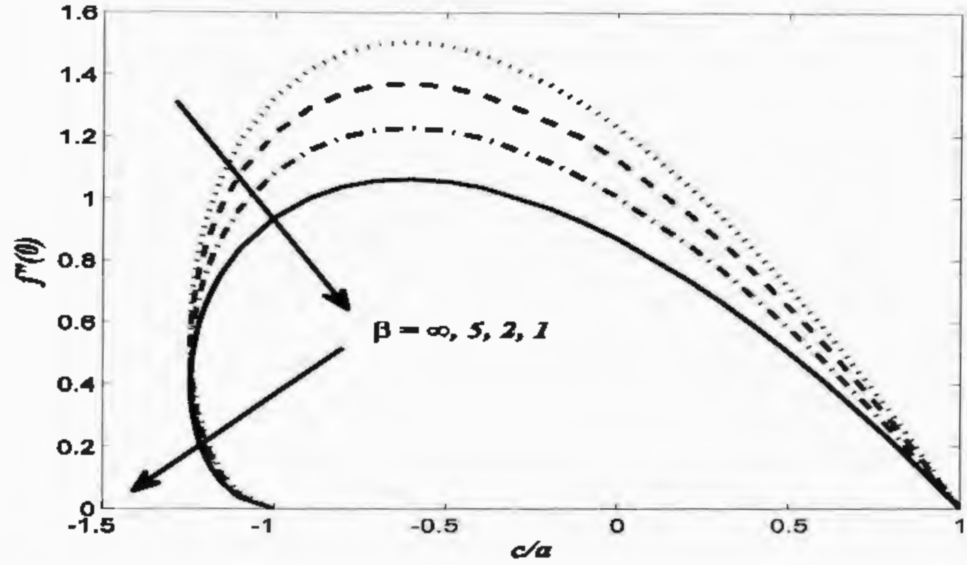


**Figure 3.2:** Graphical view of $f''(0)$ relative to $c/a$ against different $\beta$.

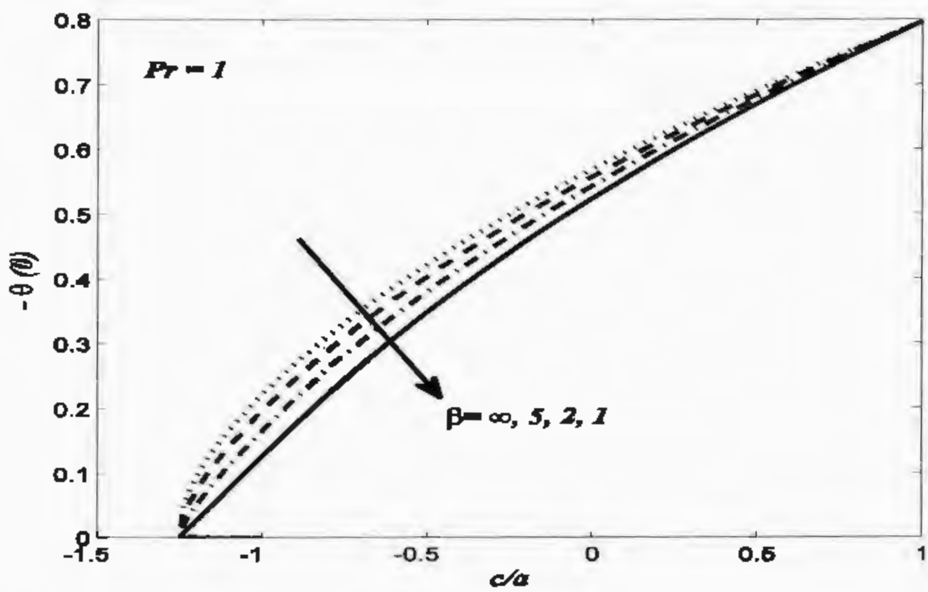


**Figure 3.3:** Graphical view of $-\theta'(0)$ relative to $c/a$ for various values of $\beta$ at $Pr=1$

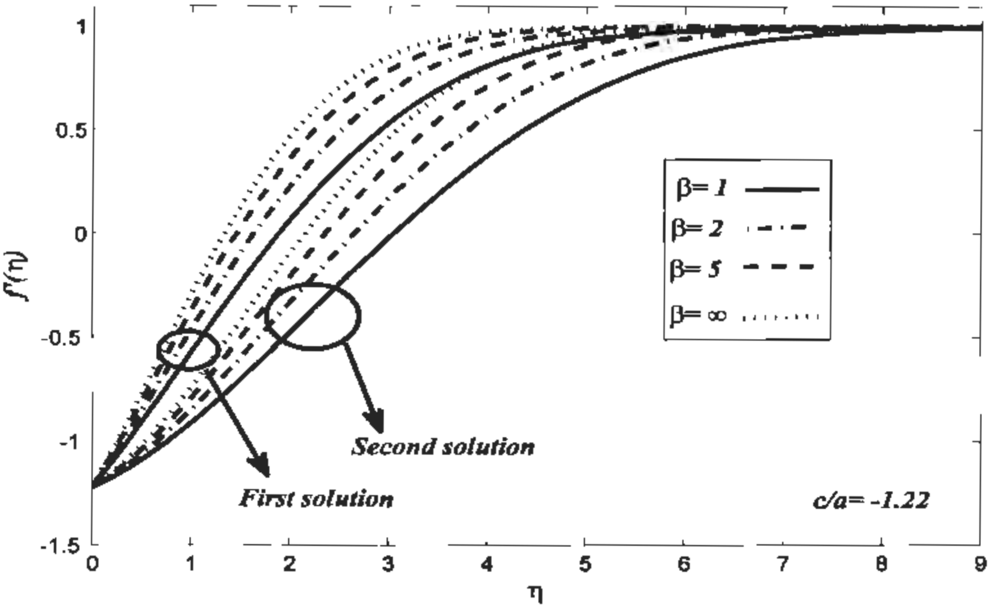


**Figure 3.4:** Graphical view of the effects shown by $\beta$ on the profile of dual velocity given by $f'(\eta)$ against $\eta$.

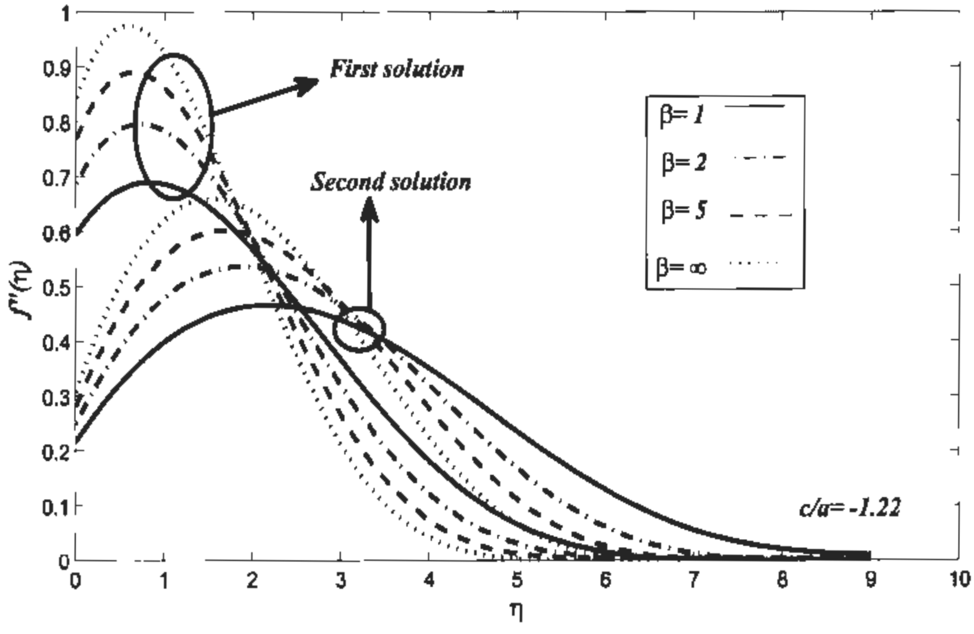


**Figure 3.5:** The influence of $\beta$ on the profile of dual velocity gradient given $f''(\eta)$ against $\eta$.

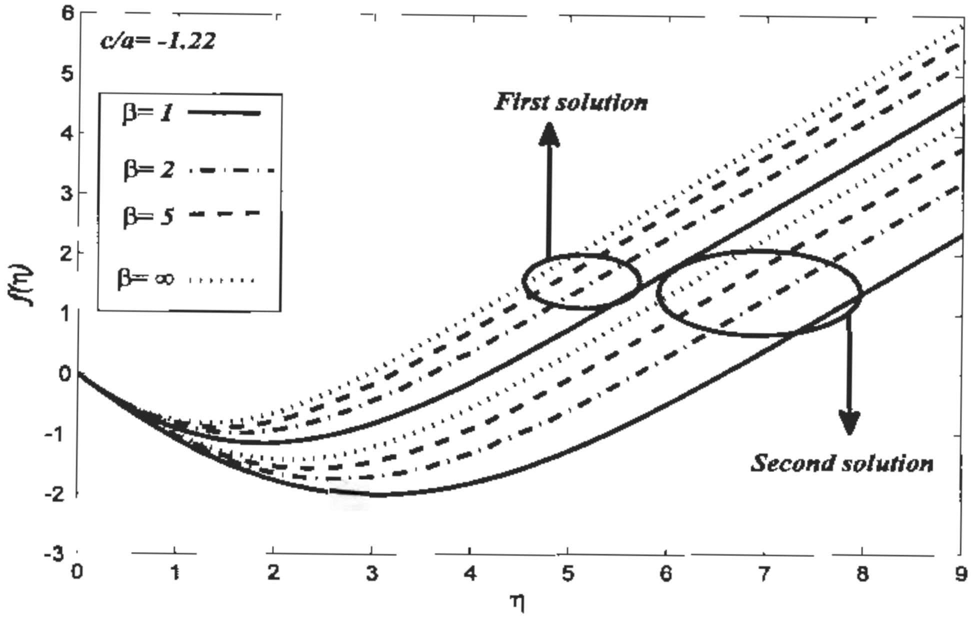


**Figure 3.6:** The effects of $\beta$ on the profile of steam function given by $f(\eta)$ against $\eta$.

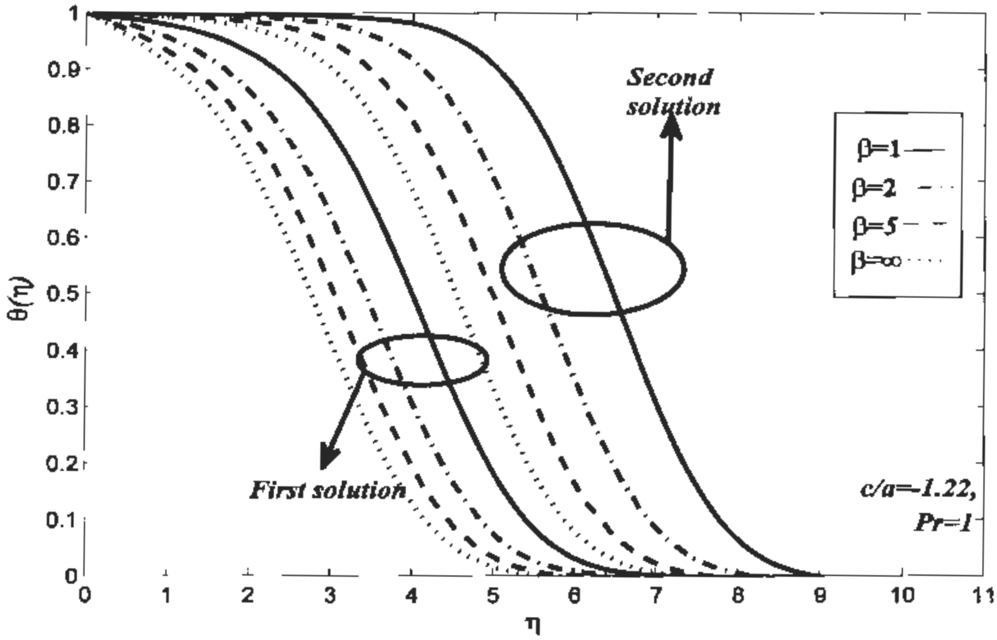


**Figure 3.7:** The effects of $\beta$ on the profile of dual temperature given by $\theta(\eta)$ against $\eta$.

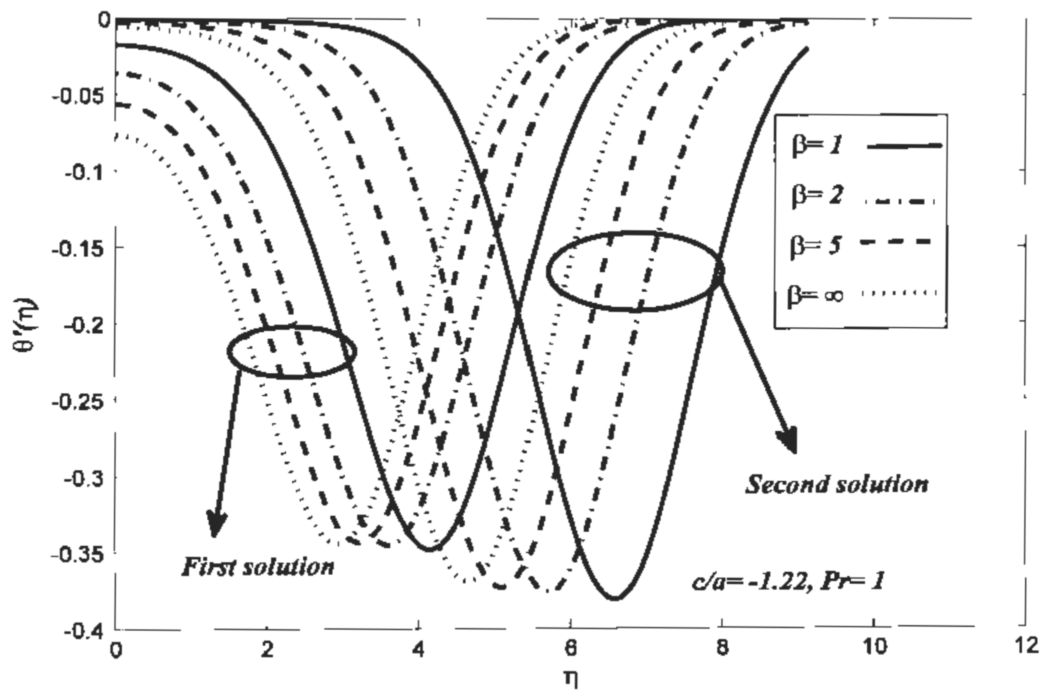


**Figure 3.8:** The effects of $\beta$ on the profile of dual temperature given by $\theta'(\eta)$ against $\eta$.

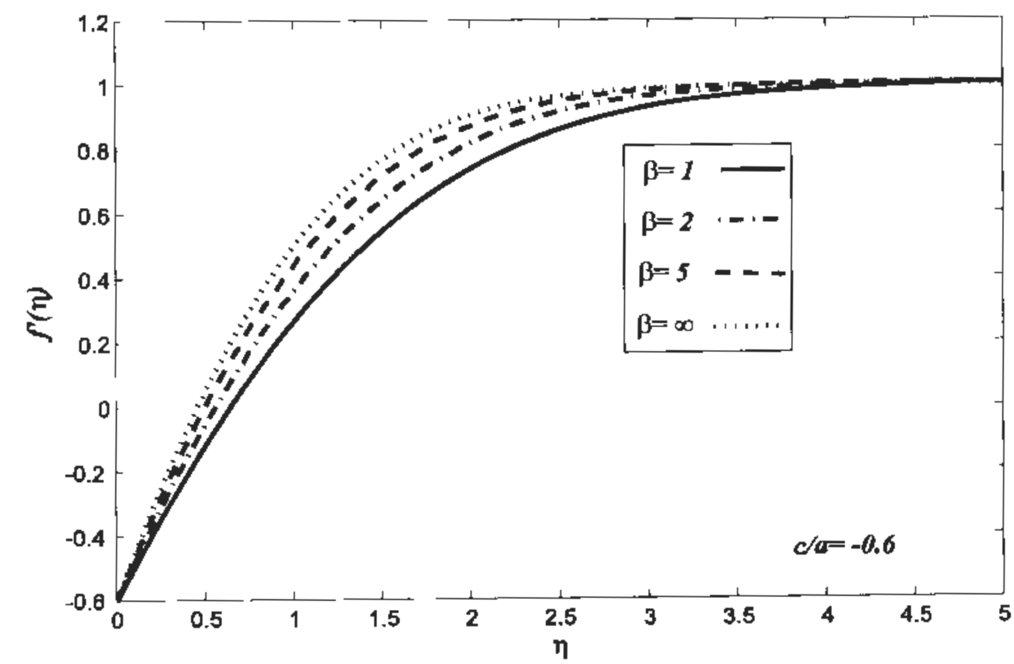


**Figure 3.9:** The influence of $\beta$ on the profile of velocity given by $f'(\eta)$ for shrinking sheet case.

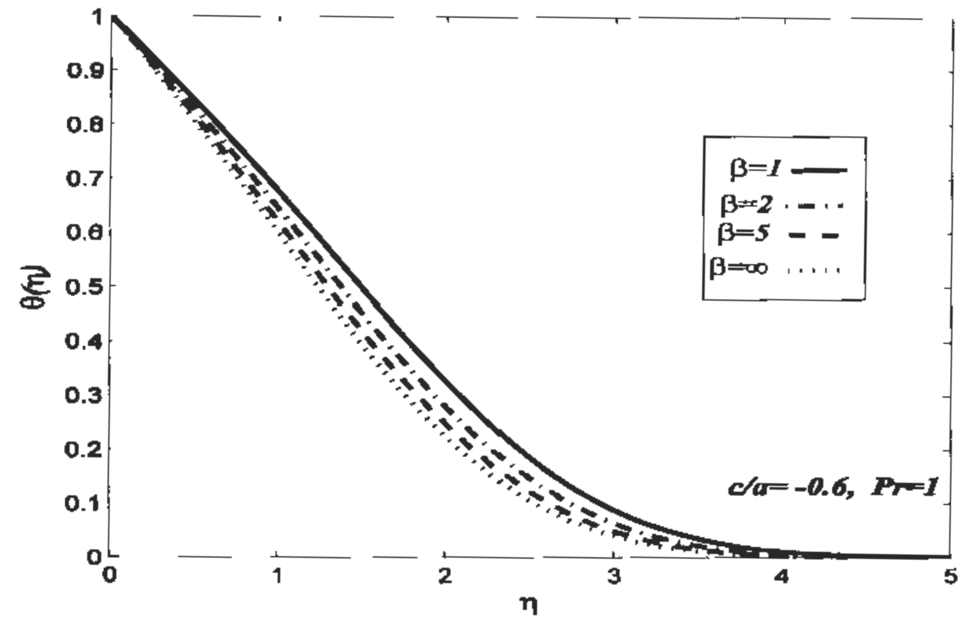


**Figure 3.10:** The influence of $\beta$ on the profile of temperature $\theta(\eta)$ for shrinking sheet case.

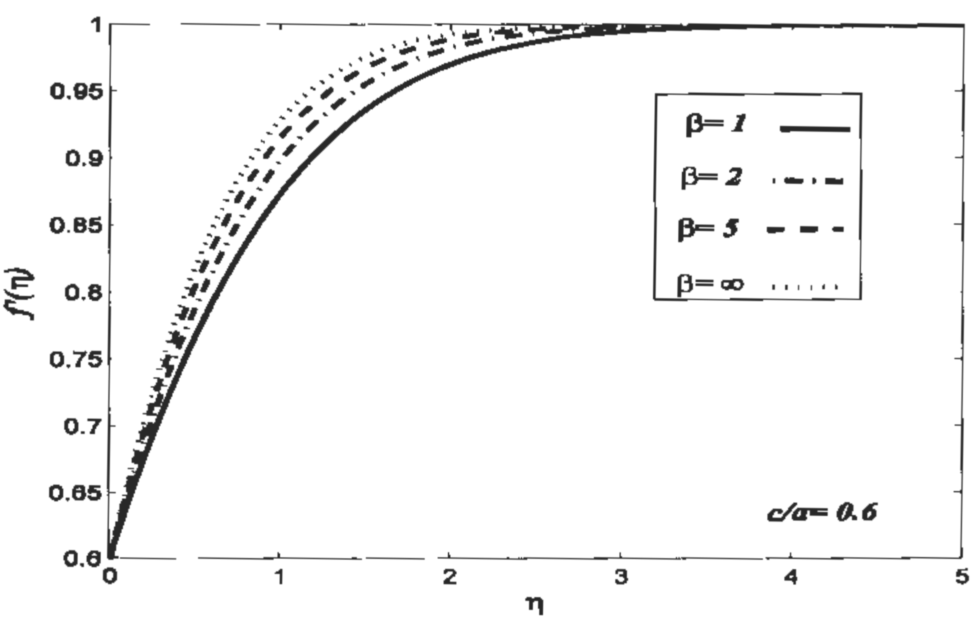


**Figure 3.11:** The influence of $\beta$ on the profile of velocity $f'(\eta)$ for stretching sheet case.

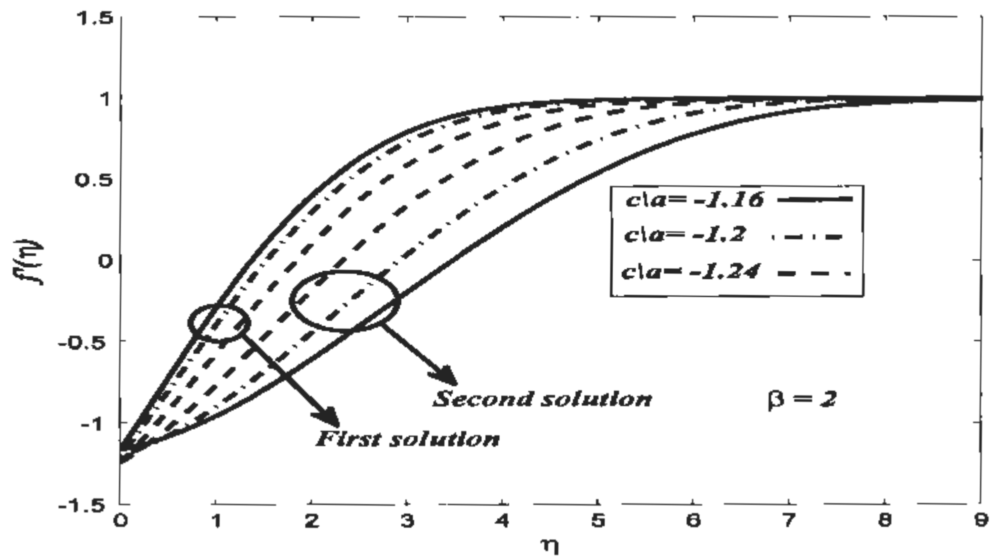


**Figure 3.12:** The influence of $c/a$ on the profile of dual velocity $f'(\eta)$ for shrinking sheet cese.

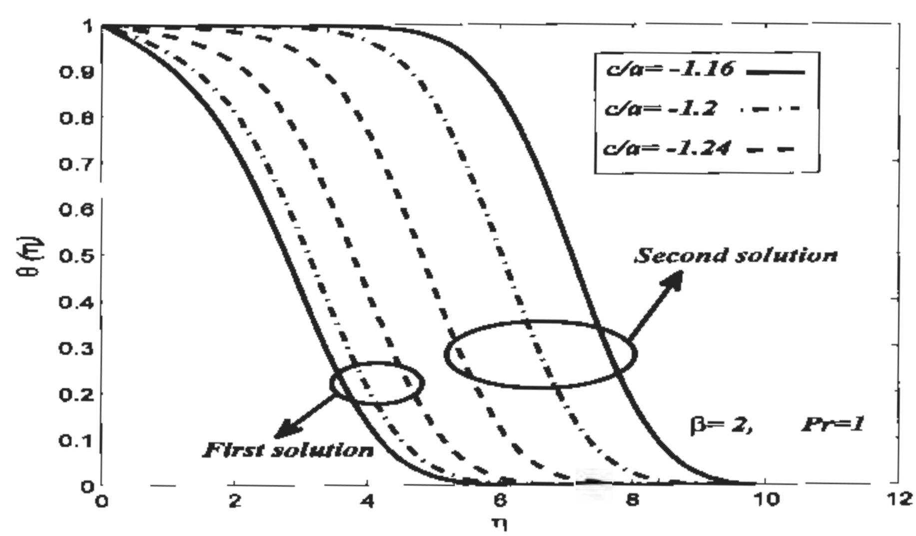


**Figure 3.13:** The influence of $c/a$ on the profile of dual temperature $\theta(\eta)$ for shrinking sheet case.

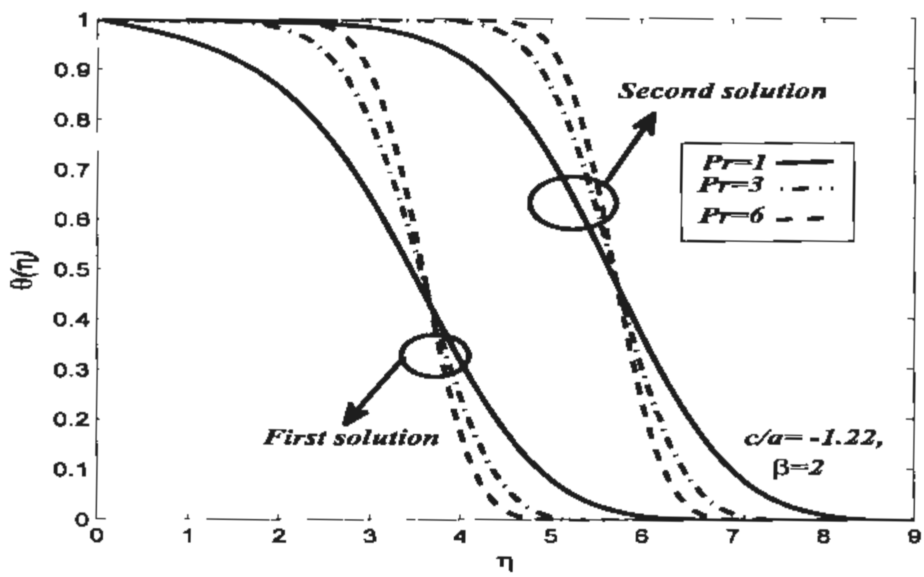


**Figure 3.14:** The influence of $Pr$ on the profile of dual temperature $\theta(\eta)$ for shrinking sheet case.

## 3.5 Results and discussion

The solution of Eq. (3.9) and Eq. (3.14) in view of boundary condition (3.10) and (3.15) are obtained by using shooting scheme for various values, assigned to the parameters i.e. Casson parameter $\beta$, velocity ratio $^{c}/_{a}$ and Prandtl number $Pr$[9]. Table 3.1 and Table 3.2 represent the comparison of the values of $f''(0)$ by present scheme with that Wang [10] and Ishak *et.al* [11] for different value of $c/a$ for stretching and shrinking sheet case. It is observed that the dual solutions exist in some situations of shrinking sheet case, the solution is unique stretching sheet case. In Figures 3.2-3.3, we show that the values of $f''(0)$ and $-\theta'(0)$ decreases with decreases in Casson parameter. Figure 3.4 shows the variation of dual solutions for some values of Casson parameter. In Fig. 3.4, we observe that the velocity is decreasing with decreasing of different values in Casson parameter for both 1st and 2nd solutions and for unique solution (Figures 3.9 & 3.11). In Figure 3.5, we indicate that velocity gradient profiles decreases with decreases in Casson parameter near the sheet, but distant from the sheet, it increases. In Figure 3.6, the stream function profile represents the back flow character of stagnation point flow over a shrinking sheet. Figure3.7, we observe that value of temperature profile increases with decreases in Casson parameter for 1st and

## References


[1] Schlichtimg, H., and Gersten, K., 2000, "Boundary layer theory" , Spinger, Berlin.

[2] Pavlov, K. B., 1974, "Magnetohydrodynamic flow of an incompressible viscous fluid caused by deformation of a surface".

[3] Bhattacharyya, K., and Layek, G.C., 2011b, "Effects of suction/blowing on steady boundary layer stagnation-point flow and heat transfer towards a shrinking sheet with thermal radiation," Int. J. Heat Mass Transfer.

[4] Crane, L.J., 1970, "Flow past a stretching plate," Z. Angew. Math. Phys

[5] Hamad, M. A. A., 2011, "Analytical solution of natural convection flow of a nanofluid over a linearly stretching sheet in the presence of magnetic field," Int. Commun. Heat Mass Transfer.

[6] Chaudhary, M. A., and Merkin, J. H., 1995, "A simple isothermal model for homogeneous-heterogeneous reactions in boundary layer flow: I.Equal Diffusivities," Fluid Dyn. Res.

[7] Cramer, K., and Pai, S., 1973, "Magnet of fluid dynamics for engineer sand applied Physicists", McGraw-Hill, NewYork.

[8] Mahapatra, T.R., and Nandy, S.K., 2013, "Stability of dual solutions in stagnation-point flow and heat transfer over a porous shrinking sheet with thermal radiation," Meccanica.

[9] Wang, C.Y., 2008, "Stagnation flow towards a shrinking sheet," Int. J. Non-Linear Mech.

[10] Ishak, A., Lok, Y.Y., and Pop, I., 2010, "Stagnation-point flow over a shrinking sheet in a micropolar fluid," Chem. Eng. Commun.

[11] Namkara, M., and Sawada, T.1988, "Numerical study on the flow of a non-Newtonian fluid through an axisymmetric stenosis", aSME J. Biomachinacal Eng.

[12] T. Y. Na, 1979, "Computational methods in engineering boundary value problems", Academic Press.

[13] Brinkman, H.C., 1952, "The Viscosity of concentrated suspensions and solution," J. Chem. Phys.

[14] Grubka, L. G., and Bobba, K. M., 1985, "Heat transfer characteristics of a continuous stretching surface with variable temperature," ASME J. Heat Transfer.

[15] Kameswaran, P.K., Narayana, M,Sibanda. P., and Murthy, P.V.S.N., 2012, "Hydromagnetic nanofluid flow due to a stretching or shrinking sheet with viscous dissipation and chemical reaction effects," Int.J.Heat Mass Transfer.

[16] Mustafa, M., Hayat, T., Pop, I. and aziz, A., 2011, "Unsteady boundary layer flow of a casson fluid due to an impulsively started moving flat plate" Heat Transferasian Res.

[17] Velagapudi, V., Konijeti, R. K.,and Aduru, C. S. K., 2008, "Empirical correlation predict thermophysical and heat transfer characteristics of nanofluids," Therm. Sci.

[18] Raj Nandkeolyar, S. S. Motsa, P. Sibanda., 2013, "Viscous and joule heating in the stagnation point nanofluid flow through a stretching sheet with homogenous–heterogeneous reactions and nonlinear convection" Journal of Nanotechnology in Engineering and Medicine

[19] Bhattacharyya, K., Hayat, T., and Alsaedi, A., 2013b, "Analytic solution for magnetohydrodynamic boundary layer flow of Casson fluid over a stretching/shrinking sheet with wall mass transfer".